Available online at www.sciencedirect.com
ScienceDirect
International Journal of Heat and Mass Transfer 51 (2008) 1024–1033
International Journal of HEAT and MASS TRANSFER
www.elsevier.com/locate/ijhmt

Radiation effects on MHD flow in a porous space

Zaheer Abbas *, Tasawar Hayat

Department of Mathematics, Quaid-I-Azam University 45320, Islamabad 44000, Pakistan

Received 8 February 2007; received in revised form 25 May 2007
Available online 12 September 2007

Abstract

This paper deals with the study of the radiation effects on the magnetohydrodynamic (MHD) flow of an incompressible viscous fluid in a porous space. The flow is induced due to a non-linear stretching sheet. Two cases of heat transfer analysis are discussed. These are: (i) the sheet with constant surface temperature (CST case) and (ii) the sheet with prescribed surface temperature (PST case). By means of similarity transformation, the governing partial differential equations are reduced into highly non-linear ordinary differential equations. The resulting non-linear system has been solved analytically using a very efficient technique namely homotopy analysis method (HAM). Expressions for velocity and temperature fields are developed in series form. Convergence of the series solution is shown explicitly. The influence of various pertinent parameters is also seen on the velocity and temperature fields. The tabulated values of the wall shear stress and the Nusselt number show good agreement with the existing results.

Keywords: Heat transfer; Non-linear stretching; Porous space; HAM solution; Electrically conducting fluid

1. Introduction

The flow of a fluid past a stretching surface is encountered in many technical and industrial applications. Some of these applications include aerodynamic extrusion of plastic sheets, the boundary layer along a material handling conveyers, cooling of an infinite metallic plate in a cooling bath, the boundary layer along a liquid film in a condensation process and heat treated material that travel between feed and wind-up rolls. After the pioneering work of Sakiadis [1], extensive literature is available on this topic for a linear stretching sheet. Some very recent contributions in this direction are made by Sadeghy et al. [2], Ariel et al. [3], Liao [4], Xu [5] and Cortell [6–8].

In all the above mentioned studies, linear stretching has been taken into account. The literature on the non-linear stretching is fairly scarce. Most recently, Cortell [9] discussed the viscous flow and heat transfer over a non-linearly stretching sheet.

The objective of the present paper is to extend the analysis of Ref. [9] in four directions (i) to consider a MHD flow (ii) to analyze the flow in a porous medium (iii) to include the radiation effects and (iv) to provide analytic solution to highly non-linear problem. A new developed powerful technique namely HAM [10,11] has been employed for the analytic solution. This technique has already been successfully applied to various problems [12–32]. Very recently, Allan [33] showed that the Adomian decomposition method is a special case of the HAM. Finally, the graphs of velocity and temperature fields are sketched and variations of sundry parameters are discussed.

2. Formulation of the problem

Let us consider the steady two-dimensional, incompressible flow of a viscous fluid with heat transfer past a flat surface coinciding with the plane $y = 0$. The wall is stretched horizontally by pulling on both sides with equal and opposite forces parallel to the wall keeping the origin fixed. The fluid is electrically conducting in the presence of a constant

* Corresponding author. Tel.: +92 51 2275341.
E-mail address: za_qau@yahoo.com (Z. Abbas).

0017-9310/$ - see front matter © 2007 Elsevier Ltd. All rights reserved.
doi:10.1016/j.ijheatmasstransfer.2007.05.031

applied magnetic field B_0 in the y-direction. The induced magnetic field is neglected using small magnetic Reynolds number assumption [34,35]. The continuity, momentum and energy equations under boundary layer approximations become

$$\frac{\partial u}{\partial x}+\frac{\partial v}{\partial y}=0, \tag{1}$$

$$u\frac{\partial u}{\partial x}+v\frac{\partial u}{\partial y}=v\frac{\partial^2 u}{\partial y^2}-\frac{\sigma B_0^2}{\rho}u-\frac{v\phi}{k}u, \tag{2}$$

$$\rho c_p\left(u\frac{\partial T}{\partial x}+v\frac{\partial T}{\partial y}\right)=k_1\frac{\partial^2 T}{\partial y^2}-\frac{\partial q_r}{\partial y}+\mu\left(\frac{\partial u}{\partial y}\right)^2, \tag{3}$$

in which u and v are the velocity components in the x- and y-directions, respectively, ρ is the fluid density, v is the kinematic viscosity, σ is the electrical conductivity, ϕ is the porosity, k is the permeability of the porous medium, T is the temperature, c_p is the specific heat, k_1 is the thermal conductivity of the fluid and q_r is the radiative heat flux.

Using the Rosseland approximation for radiation for an optically thick layer [36] one can obtain

$$q_r=-\frac{4\sigma^*}{3k^*}\frac{\partial T^4}{\partial y}, \tag{4}$$

where σ^* is the Stefan–Boltzmann constant and k^* is the mean absorption coefficient. We express the term T^4 as a linear function of temperature in a Taylor series about T_∞ and neglecting higher terms, therefore we have

$$T^4\cong 4T_\infty^3T-3T_\infty^4. \tag{5}$$

From Eqs. (3)–(5) we can write

$$\rho c_p\left(u\frac{\partial T}{\partial x}+v\frac{\partial T}{\partial y}\right)=\frac{\partial}{\partial y}\left[\left(\frac{16\sigma^*}{3k^*}+k_1\right)\frac{\partial T}{\partial y}\right]+\mu\left(\frac{\partial u}{\partial y}\right)^2. \tag{6}$$

The appropriate boundary conditions are

$$u_w(x)=Cx^n,\quad v=0\quad \text{at}\quad y=0, \tag{7}$$

$$u\to 0\quad \text{as}\quad y\to\infty, \tag{8}$$

where C and n are parameters related to the surface stretching speed.

For temperature we have the following two sets of boundary conditions.

Case a: Constant surface temperature (CST)

$$\begin{aligned}&T=T_w\quad \text{at}\quad y=0,\\ &T\to T_\infty\quad \text{as}\quad y\to\infty.\end{aligned} \tag{9}$$

Case b: Prescribed surface temperature (PST)

$$\begin{aligned}&T=T_w\left(=T_\infty+Ax^K\right)\quad \text{at}\quad y=0,\\ &T\to T_\infty\quad \text{as}\quad y\to\infty,\end{aligned} \tag{10}$$

where K is the surface temperature parameter.

Defining the following non-dimensionlized quantities:

$$\begin{aligned}&\eta=y\sqrt{\frac{C(n+1)}{2v}},\quad u=Cx^nf'(\eta),\\ &v=-\sqrt{\frac{Cv(n+1)}{2}}x^{\frac{n-1}{2}}\left[f(\eta)+\frac{n-1}{n+1}\eta f'(\eta)\right],\\ &\theta(\eta)=\frac{T-T_\infty}{T_w-T_\infty},\end{aligned} \tag{11}$$

continuity Eq. (1) is satisfied automatically and Eqs. (2) and (7) become

$$f'''+ff''-\frac{2n}{n+1}f'^2-M^2f'-\lambda f'=0, \tag{12}$$

$$f(0)=0,\quad f'(0)=1,\quad f'(\infty)=0. \tag{13}$$

The shear stress at the stretched surface is

$$\tau_w=\mu\left(\frac{\partial u}{\partial y}\right)_w, \tag{14}$$

which in non-dimensional form becomes

$$\tau_w=C\mu\sqrt{\frac{C(n+1)}{2v}}x^{\frac{3n-1}{2}}f''(0). \tag{15}$$

For temperature with the help of Eqs. (6) and (9)–(11) we get:

Case a: Constant surface temperature (CST)

$$\left(1+\frac{4}{3}R_d\right)\theta''+Prf\theta'+PrEcf''^2=0, \tag{16}$$

$$\theta(0)=1,\quad \theta(\infty)=0 \tag{17}$$

and the rate of heat transfer of the surface is

$$-\lambda_T\left(\frac{dT}{dy}\right)_{y=0}=-\lambda_T(T_w-T_\infty)\left(1+\frac{4}{3}R_d\right)\theta'(0)x^{\frac{n-1}{2}}\times\sqrt{\frac{C(n+1)}{2v}}. \tag{18}$$

Case b: Prescribed surface temperature (PST)

$$\left(1+\frac{4}{3}R_d\right)\theta''+Prf\theta'-\left(\frac{2K}{n+1}\right)Prf'\theta+PrEc'x^{2n-K}f''^2=0. \tag{19}$$

The above equation for $K=2n$ reduces to

$$\left(1+\frac{4}{3}R_d\right)\theta''+Prf\theta'-\left(\frac{4n}{n+1}\right)Prf'\theta+PrEc'f''^2=0, \tag{20}$$

$$\theta(0)=1,\quad \theta(\infty)=0. \tag{21}$$

and the local surface heat flux is

$$q_w=-\lambda_T\left(\frac{dT}{dy}\right)_w=-\lambda_TAx^{\frac{2K+n-1}{2}}\left(1+\frac{4}{3}R_d\right)\theta'(0)\sqrt{\frac{C(n+1)}{2v}}. \tag{22}$$

Here the local Hartmen number M, the local porosity parameter λ, the Prandtl number Pr, the Eckert number Ec, the radiation parameter R_d and Ec' are respectively

$$M^2=\frac{2x^{n-1}\sigma B_0^2}{C\rho(n+1)},\quad \lambda=\frac{2x^{n-1}\nu\phi}{Ck(n+1)},\quad Pr=\frac{\mu c_p}{k_1},$$
$$Ec=\frac{u_w^2}{c_p(T_w-T_\infty)},\quad R_d=\frac{4\sigma^* T_\infty^3}{k^* k_1},\quad Ec'=\frac{C^2}{Ac_p}.$$

In the next two sections, we will solve the non-linear systems consisting of Eqs. (12), (13), (16), (17), (20) and (21) by HAM.

3. Analytic solution for velocity $f(\eta)$

For HAM solution of Eqs. (12) and (13), it is straightforward to choose the initial approximation

$$f_0(\eta)=1-\exp(-\eta) \tag{23}$$

and the auxiliary linear operator

$$\mathscr{L}_1(f)=f'''-f', \tag{24}$$

with the following property

$$\mathscr{L}_1[C_1+C_2e^{\eta}+C_3e^{-\eta}]=0, \tag{25}$$

in which C_i, $i=1-3$ are arbitrary constants. If $p\,(\in[0\,1])$ and $\hbar_1$ indicate the embedding and non-zero auxiliary parameters, respectively then we have:

The zeroth-order deformation problem

$$(1-p)\mathscr{L}_1\left[\widehat{f}(\eta;p)-f_0(\eta)\right]=p\hbar_1\mathscr{N}_1\left[\widehat{f}(\eta;p)\right], \tag{26}$$

$$\widehat{f}(0;p)=0,\quad \widehat{f}'(0;p)=1,\quad \widehat{f}'(\infty;p)=0. \tag{27}$$

The mth-order deformation problem

$$\mathscr{L}_1[f_m(\eta)-\chi_m f_{m-1}(\eta)]=\hbar_1\mathscr{R}_{1m}(\eta), \tag{28}$$
$$f_m(0)=f_m'(0)=f_m'(\infty)=0, \tag{29}$$

where

$$\mathscr{N}_1\left[\widehat{f}(\eta;p)\right]=\frac{\partial^3\widehat{f}(\eta;p)}{\partial\eta^3}+\widehat{f}(\eta;p)\frac{\partial^2\widehat{f}(\eta;p)}{\partial\eta^2}-\frac{2n}{n+1}\left(\frac{\partial\widehat{f}(\eta;p)}{\partial\eta}\right)^2-M^2\frac{\partial\widehat{f}(\eta;p)}{\partial\eta}-\lambda\frac{\partial\widehat{f}(\eta;p)}{\partial\eta}, \tag{30}$$

$$\mathscr{R}_{1m}(\eta)=f_{m-1}'''(\eta)-M^2f_{m-1}'-\lambda f_{m-1}'+\sum_{k=0}^{m-1}\left[f_{m-1-k}f_k''-\frac{2n}{n+1}f_{m-1-k}'f_k'\right], \tag{31}$$

$$\chi_m=\begin{cases}0, & m\leqslant 1,\\ 1, & m>1.\end{cases} \tag{32}$$

Now using Mathematics one can solve Eqs. (28) and (29) up to first few order of approximations. The forms of Eqs. (28) and (29) give us the following type of solution of f_m:

$$f_m(\eta)=\sum_{n=0}^{m+1}\sum_{q=0}^{m+1-n}a_{m,n}^q\eta^q e^{-n\eta},\quad m\geqslant 0, \tag{33}$$

where the recurrence formulas for the coefficients $a_{m,n}^k$ of $f_m(\eta)$ are obtained for $m\geqslant 1$, $0\leqslant n\leqslant m+1$ and $0\leqslant k\leqslant m+l-n$ as

$$a_{m,0}^0=\chi_m\chi_{m+2}a_{m-1,0}^0-\sum_{q=0}^{m}\Delta_{m,1}^q\mu_{1,1}^q-\sum_{n=2}^{m+1}\sum_{q=1}^{m+1-n}\Delta_{m,n}^q\{\mu_{n,1}^q-(n-1)\mu_{n,0}^q\},$$

$$a_{m,0}^k=\chi_m\chi_{m+2-k}a_{m-1,0}^k,\quad 0\leqslant k\leqslant m+1,$$

$$a_{m,1}^0=\chi_m\chi_{m+1}a_{m-1,1}^0+\sum_{q=0}^{m}\Delta_{m,1}^q\mu_{1,1}^q-\sum_{n=2}^{m+1}\left[n\Delta_{m,n}^0\mu_{n,0}^0+\sum_{q=1}^{m+1-n}\Delta_{m,n}^q\left(n\mu_{n,0}^q-\mu_{n,1}^q\right)\right],$$

$$a_{m,1}^k=\chi_m\chi_{m+1-k}a_{m-1,1}^k-\sum_{q=k-1}^{m}\Delta_{m,1}^q\mu_{1,k}^q,\ 1\leqslant k\leqslant 2m+1,$$

$$a_{m,n}^k=\chi_m\chi_{m+2-n-k}a_{m-1,n}^k-\sum_{q=k}^{m+1-n}\Delta_{m,n}^q\mu_{n,k}^q,$$

$$2\leqslant n\leqslant m+1,\ 0\leqslant k\leqslant m+1-n,$$

$$\mu_{1,k}^q=\sum_{p=0}^{q+1-k}\frac{q!}{k!2^{q+1-k-p}},\quad q\geqslant 0,\ 1\leqslant k\leqslant q+1, \tag{34}$$

$$\mu_{n,k}^q=\sum_{r=0}^{q-k}\sum_{p=0}^{q-k-r}\frac{q!}{k!(n-1)^{q+1-k-r-p}n^{r+1}(n+1)^{p+1}},\quad q\geqslant 0,\ 1\leqslant k\leqslant q,\ n\geqslant 2, \tag{35}$$

$$\Delta_{m,n}^q=\hbar_1\left[\chi_{m-n-q+2}\left(e_{m-1,n}^q-(M^2+\lambda)c_{m-1,n}^q\right)+\left(\alpha_{m,n}^q-\frac{2n}{n+1}\beta_{m,n}^q\right)\right]. \tag{36}$$

The coefficients $\alpha_{m,n}^q$ and $\beta_{m,n}^q$, where $m\geqslant 1$, $0\leqslant n\leqslant m+1$, $0\leqslant q\leqslant m+1-n$ are

$$\alpha_{m,n}^q=\sum_{k=0}^{m-1}\sum_{j=\max\{0,n-m+k\}}^{\min\{n,k+1\}}\sum_{i=\max\{0,q-m+k+n-j\}}^{\min\{q,k+1-j\}}d_{k,j}^i a_{m-1-k,n-j}^{q-i},$$

$$\beta_{m,n}^q=\sum_{k=0}^{m-1}\sum_{j=\max\{0,n-m+k\}}^{\min\{n,k+1\}}\sum_{i=\max\{0,q-m+k+n-j\}}^{\min\{q,k+1-j\}}c_{k,j}^i c_{m-1-k,n-j}^{q-i},$$

$$c_{m,n}^k=(k+1)a_{m,n}^{k+1}-na_{m,n}^k,$$

$$d_{m,n}^k=(k+1)c_{m,n}^{k+1}-nc_{m,n}^k,$$

$$e_{m,n}^k=(k+1)d_{m,n}^{k+1}-nd_{m,n}^k.$$

For the detailed procedure of deriving the above relations the reader is referred to [11]. Using the above recurrence formulas, we can calculate all coefficients $a_{m,n}^k$ using only the first few

$$a_{0,0}^0=1,\quad a_{0,0}^1=0,\quad a_{0,1}^0=-1, \tag{37}$$

given by the initial guess approximation in Eq. (23).

The explicit, totally analytic solution is

$$f(\eta)=\sum_{m=0}^{\infty} f_m(\eta) = \lim_{M\to\infty}\left[\sum_{m=0}^{M} a_{m,0}^{0}+\sum_{n=1}^{M+1}\mathrm{e}^{-n\eta}\left(\sum_{m=n-1}^{M}\sum_{k=0}^{m+1-n} a_{m,n}^{k}\eta^{k}\right)\right]. \tag{38}$$

4. Analytic solutions for temperature $\theta(\eta)$

Case a: Constant surface temperature (CST)

To seek the analytic solution of Eqs. (16) and (17) using HAM, we take the initial guess approximation of $\theta(\eta)$ and auxiliary linear operator as

$$\theta_0(\eta)=\exp(-\eta), \tag{39}$$

$$\mathscr{L}_2(f)=f''-f, \tag{40}$$

with

$$\mathscr{L}_2[C_4\mathrm{e}^{\eta}+C_5\mathrm{e}^{-\eta}]=0, \tag{41}$$

in which C_4 and C_5 are the arbitrary constants. If $\hbar_2$ indicates the non-zero auxiliary parameter then we get:

The zeroth-order deformation problem

$$(1-p)\mathscr{L}_2\left[\widehat{\theta}(\eta;p)-\theta_0(\eta)\right]=p\hbar_2\mathscr{N}_2\left[\widehat{\theta}(\eta;p),\widehat{f}(\eta;p)\right], \tag{42}$$

$$\widehat{\theta}(0;p)=1,\quad \theta(\infty;p)=0, \tag{43}$$

in which the non-linear operator $\mathscr{N}_2$ is

$$\mathscr{N}_2\left[\widehat{\theta}(\eta;p),\widehat{f}(\eta;p)\right]=\left(1+\frac{4}{3}R_d\right)\frac{\partial^2\widehat{\theta}(\eta;p)}{\partial\eta^2}+Pr\widehat{f}(\eta;p)\frac{\partial\widehat{\theta}(\eta;p)}{\partial\eta}+PrEc\left(\frac{\partial^2\widehat{f}(\eta;p)}{\partial\eta^2}\right)^2, \tag{44}$$

and

The mth-order deformation problem

$$\mathscr{L}_2[\theta_m(\eta)-\chi_m\theta_{m-1}(\eta)]=\hbar_2\mathscr{R}_{2m}(\eta), \tag{45}$$

$$\theta_m(0)=\theta_m(\infty)=0, \tag{46}$$

$$\mathscr{R}_{2m}(\eta)=\left(1+\frac{4}{3}R_d\right)\theta''_{m-1}(\eta)+Pr\sum_{k=0}^{m-1}\left[\theta'_{m-1-k}f_k+Ecf''_{m-1-k}f''_k\right]. \tag{47}$$

Using the software Mathematica one can solve Eqs. (45) and (46) up to first few order of approximations. We get the following type of solution of θ_m:

$$\theta_m(\eta)=\sum_{n=0}^{m+1}\sum_{q=0}^{m+1-n} b_{m,n}^{q}\eta^{q}\mathrm{e}^{-n\eta},\quad m\geqslant 0, \tag{48}$$

where the recurrence formulas for the coefficients $b_{m,n}^{k}$ of $\theta_m(\eta)$ are obtained for $m\geqslant 1$, $0\leqslant n\leqslant m+1$ and $0\leqslant k\leqslant m+1-n$ as

$$b_{m,0}^{k}=\chi_m\chi_{m+2-k}b_{m-1,0}^{k}+\sum_{q=0}^{m+1}\Gamma_{m,0}^{q}\mu 1_{1,0}^{q},$$

$$b_{m,1}^{0}=\chi_m\chi_{m+1}b_{m-1,1}^{0}-\sum_{q=0}^{m+1}\Gamma_{m,0}^{q}\mu 1_{0,0}^{q}-\sum_{n=2}^{m+1}\sum_{q=0}^{m+1-n}\Gamma_{m,n}^{q}\mu 1_{n,0}^{q},$$

$$b_{m,1}^{k}=\chi_m\chi_{m+1-k}b_{m-1,1}^{k}+\sum_{q=k-1}^{m}\Gamma_{m,1}^{q}\mu 1_{1,k}^{q},\quad 1\leqslant k\leqslant m+1,$$

$$b_{m,n}^{k}=\chi_m\chi_{m+2-n-k}b_{m-1,n}^{k}+\sum_{q=k}^{m+1-n}\Gamma_{m,n}^{q}\mu 1_{n,k}^{q},\ 2\leqslant n\leqslant m+1,\ 0\leqslant k\leqslant m+1-n,$$

$$\mu 1_{1,k}^{q}=\frac{(-1)^{2q+1-2k-p}q!}{2^{q+2-k}k!},\ q\geqslant 0,\ 0\leqslant k\leqslant q+1, \tag{49}$$

$$\mu 1_{n,k}^{q}=\sum_{p=0}^{q+1-k}\frac{q!}{k!(n+1)^{p+1}(n-1)^{q+1-k-p}},\quad q\geqslant 0,\ 1\leqslant k\leqslant q,\ n\geqslant 2, \tag{50}$$

$$\Gamma_{m,n}^{q}=\hbar_2\left[\chi_{m-n-q+1}\left(1+\frac{4}{3}Rd\right)g_{m-1,n}^{q}+Pr\left(\gamma_{m,n}^{q}+Ec\delta_{m,n}^{q}\right)\right]. \tag{51}$$

The coefficients $\gamma_{m,n}^{q}$ and $\delta_{m,n}^{q}$, where $m\geqslant 1$, $0\leqslant n\leqslant m+1$, $0\leqslant q\leqslant m+1-n$ are

$$\gamma_{m,n}^{q}=\sum_{k=0}^{m-1}\sum_{j=\max\{0,n-m+k\}}^{\min\{n,k+1\}}\sum_{i=\max\{0,q-m+k+n-j\}}^{\min\{q,k+1-j\}} a_{k,j}^{i}f_{m-1-k,n-j}^{q-i},$$

$$\delta_{m,n}^{q}=\sum_{k=0}^{m-1}\sum_{j=\max\{0,n-m+k\}}^{\min\{n,k+1\}}\sum_{i=\max\{0,q-m+k+n-j\}}^{\min\{q,k+1-j\}} d_{k,j}^{i}d_{m-1-k,n-j}^{q-i},$$

$$f_{m,n}^{k}=(k+1)b_{m,n}^{k+1}-nb_{m,n}^{k},$$

$$g_{m,n}^{k}=(k+1)f_{m,n}^{k+1}-nf_{m,n}^{k},$$

Employing the above recurrence formulas, we can calculate all coefficients $b_{m,n}^{k}$ using only

$$b_{0,0}^{0}=b_{0,0}^{1}=0,\quad b_{0,1}^{0}=1, \tag{52}$$

given by the initial guess approximations in Eq. (39) and thus the temperature field is

$$\theta(\eta)=\sum_{m=0}^{\infty}\theta_m(n)=\lim_{M\to\infty}\left[\sum_{m=0}^{M}b^0_{m,0}+\sum_{n=1}^{M+1}e^{-n\eta}\left(\sum_{m=n-1}^{M}\sum_{k=0}^{m+1-n}b^k_{m,n}\eta^k\right)\right]. \tag{53}$$

Case b: Prescribed surface temperature (PST)

Employing the same methodology as in case (a), the solution here is

$$\theta(\eta)=\sum_{m=0}^{\infty}\theta_m(n)=\lim_{M\to\infty}\left[\sum_{m=0}^{M}b^0_{m,0}+\sum_{n=1}^{M+1}\mathrm{e}^{-m\eta}\left(\sum_{m=n-1}^{M}\sum_{k=0}^{m+1-n}b^k_{m,n}\eta^k\right)\right], \tag{54}$$

where

$$\mathscr{N}_2\left[\widehat{\theta}(\eta;p),\widehat{f}(\eta;p)\right]=\left(1+\frac{4}{3}R_d\right)\frac{\partial^2\widehat{\theta}(\eta;p)}{\partial\eta^2}+Pr\widehat{f}(\eta;p)\frac{\partial\widehat{\theta}(\eta;p)}{\partial\eta}-\left(\frac{2K}{n+1}\right)Pr\widehat{\theta}(\eta;p)\frac{\partial\widehat{f}(\eta;p)}{\partial\eta}+PrEc'\left(\frac{\partial^2\widehat{f}(\eta;p)}{\partial\eta^2}\right)^2, \tag{55}$$

$$\mathscr{R}_{3m}(\eta)=\left(1+\frac{4}{3}R_d\right)\theta'''_{m-1}(\eta)+Pr\sum_{k=0}^{m-1}\left[\theta'_{m-1-k}f_k-\left(\frac{2K}{n+1}\right)\theta_{m-1-k}f'_k+Ec'f'''_{m-1-k}f'_k\right] \tag{56}$$

$$\Pi^q_{m,n}=\hbar_2\left[\chi_{m-n-q+2}\left(1+\frac{4}{3}Rd\right)g^q_{m-1,n}+Pr\left(\gamma^q_{m,n}-\left(\frac{2K}{n+1}\right)\omega^q_{m,n}+Ec'\delta^q_{m,n}\right)\right], \tag{57}$$

$$\omega^q_{m,n}=\sum_{k=0}^{m-1}\sum_{j=\max\{0,n-m+k\}}^{\min\{n,k+1\}}\sum_{i=\max\{0,q-m+k+n-j\}}^{\min\{q,k+1-j\}}c^i_{k,j}b^{q-i}_{m-1-k,n-j}.$$

Putting $\Pi^q_{m,n}$ instead of $\Gamma^q_{m,n}$ in case (a), we can get the formulas for the coefficients $b^k_{m,n}$ for case (b).

5. Convergence of the HAM solution

As pointed out by Liao [10], the convergence and rate of approximation for the HAM solutions, i.e., the series (38), (53) and (54) are strongly dependent upon $\hbar_1$ and $\hbar_2$. In order to find the admissible values of $\hbar_1$ and $\hbar_2$, $\hbar$-curves are plotted for 25th-order of approximations. It is obvious from Fig. 1 that the range for the admissible values of $\hbar_1$ and $\hbar_2$ are $-1.05\leqslant\hbar_1\leqslant-0.1$ and $-1.5\leqslant\hbar_2\leqslant-0.2$. Our computations show that the series (38), (53) and (54) converge in the whole region of η when $\hbar_1=-0.6$ and $\hbar_2=-0.8$.

6. Results and discussion

This section describes the influence of some interesting parameters on the velocity and temperature fields. In particular, attention has been focused to the variations of n, the Hartman number M, porosity parameter λ, Prandtl number Pr, Eckert number Ec, Ec', and the radiation parameter R_d on the velocity and temperature fields, respectively. Moreover, the values of the wall shear stress $-f''(0)$ and the Nusselt number $-\theta'(0)$ are computed in the Tables 1–4.

In order to see the effects of n, the Hartman number M and the porosity parameter λ on the velocity component f', we prepared Figs. 2–4. Fig. 2 depicts the effects of n on f'. It shows that the velocity is a decreasing function of n. Figs. 3 and 4 describe the effects of M and λ on f', respectively. It is noted that velocity f' is an increasing function of M and λ. But this increment, is larger in a porous medium.

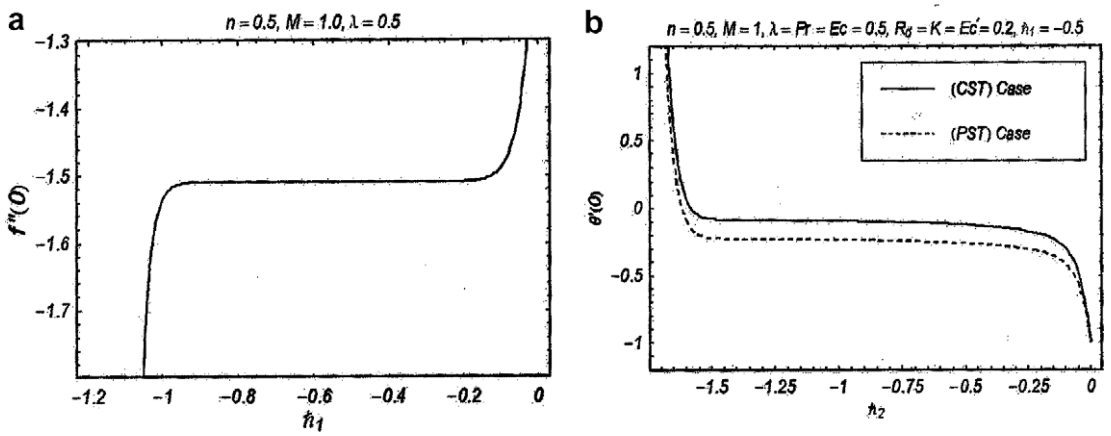

Fig. 1. $\hbar$-curves for 25th-order approximations.

Table 1
Values of the wall shear stress $-f''(0)$ when $M = \lambda = 0$

n	Cortell [9]	HAM solution
0.0	0.627547	0.627547
0.2	0.766758	0.766837
0.5	0.889477	0.889544
0.75	0.953786	0.953956
1.0	1.0	1.0
1.5	1.061587	1.061601
3.0	1.148588	1.148593
7.0	1.216847	1.216851
10.0	1.234875	1.234874
20.0	1.257418	1.257423
100.0	1.276768	1.276773

Table 2
Values of the wall shear stress $-f''(0)$ in the presence of M and λ

n	M	λ	$-f''(0)$	n	M	λ	$-f''(0)$
0.0	0.5	0.5	1.052407	1.5	0.0	0.5	1.276454
0.2			1.148901		0.2		1.292071
0.5			1.238663		0.5		1.371113
0.75			1.287402		0.7		1.456154
1.0			1.322875		1.0		1.622041
1.5			1.371113		2.0		2.373247
3.0			1.440650		0.5	0.0	1.174068
7.0			1.496283			0.2	1.256655
10.0			1.511120			0.5	1.371113
20.0			1.529766			0.7	1.442332
100.0			1.545838			1.0	1.542966

Figs. 5–10 are made for the effects of n, M, λ, Pr, Ec and R_d on the temperature field θ in CST (Constant surface temperature) case. Fig. 5 shows that θ increases for large values of n. Figs. 6 and 7 illustrate the effects of M and λ on θ. The temperature profile θ increases as M and λ increase, respectively. But this increment in case of M is larger when compared with λ. Fig. 8 elucidates the variation of Pr on temperature θ. It is observed that θ decreases as Pr increases. Fig. 9 gives the behavior of Ec on θ. It is noted that θ has opposite results when compared with Fig. 8. Fig. 10 shows the effects of radiation parameter R_d on θ. It is obvious from Fig. 10 that the temperature θ is an increasing function of R_d.

Figs. 11–16 are plotted for the effects of n, M, λ, Pr, Ec' and R_d, on the temperature field θ in PST (Prescribed surface temperature) case. Fig. 11 depicts the effects of n on θ. It has the similar results when compared with Fig. 5 in (CST) case. Figs. 12 and 13 show the influence of M and λ on θ, respectively. It is found that these Figs. have the similar results as in Figs. 6 and 7 for (CST) case. Fig. 14 indicates that θ is a decreasing function of Pr. But this decrement is larger when compared with Fig. 8. Fig. 15 shows that θ increases as Ec' increases. Fig. 16 elucidates the effects of R_d on θ. It is noted that θ is increased when R_d increases. The change in Fig. 16 is larger when compared with Fig. 10.

Table 3
Heat transfer characteristics at the wall $-\theta'(0)$ for CST case when $M = \lambda = R_d = 0$

		Cortell [9]	HAM solution	Cortell [9]	HAM solution
Ec	n	$Pr = 1$	$Pr = 1$	$Pr = 5$	$Pr = 5$
0.0	0.2	0.610262	0.610217	1.607175	1.607925
	0.5	0.595277	0.595201	1.586744	1.586833
	1.5	0.574537	0.574729	1.557463	1.557672
	3.0	0.564472	0.564661	1.542337	1.542145
	10.0	0.554960	0.554878	1.528573	1.528857
0.1	0.2	0.574985	0.574955	1.474764	1.474203
	0.5	0.556623	0.556775	1.436789	1.437242
	1.5	0.530966	0.530962	1.381861	1.382003
	3.0	0.517977	0.518043	1.352768	1.352548
	10.0	0.505121	0.505127	1.324772	1.324943

Table 4
Heat transfer characteristics at the wall $-\theta'(0)$ for PST case when $K = 2n$ at $M = \lambda = R_d = 0$

		Cortell [9]	HAM solution	Cortell [9]	HAM solution
Ec'	n	$Pr = 1$	$Pr = 1$	$Pr = 5$	$Pr = 5$
0.0	0.75	1.252672	1.252700	3.124975	3.124347
	1.5	1.439393	1.439375	3.567737	3.567944
	7.0	1.699298	1.699318	4.185373	4.185378
	10.0	1.728934	1.728952	4.255972	4.255935
0.1	0.75	1.219985	1.219940	3.016983	3.016934
	1.5	1.405078	1.405184	3.455721	3.455875
	7.0	1.662506	1.662599	4.065722	4.065791
	10.0	1.691822	1.691812	4.135296	4.135299

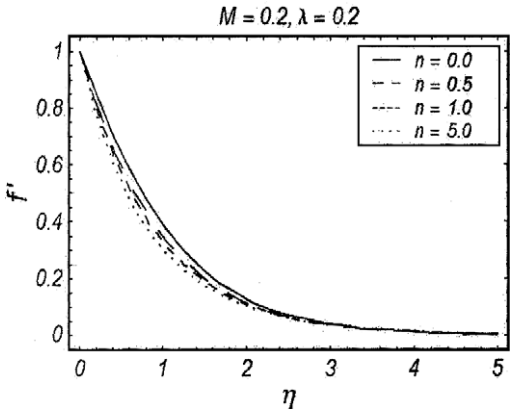

Fig. 2. Effects of n on f' at $\hbar_1 = -0.6$.

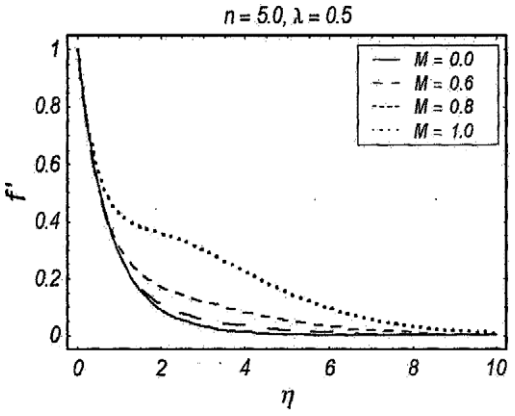

Fig. 3. Effects of M on f' at $\hbar_1 = -0.6$.

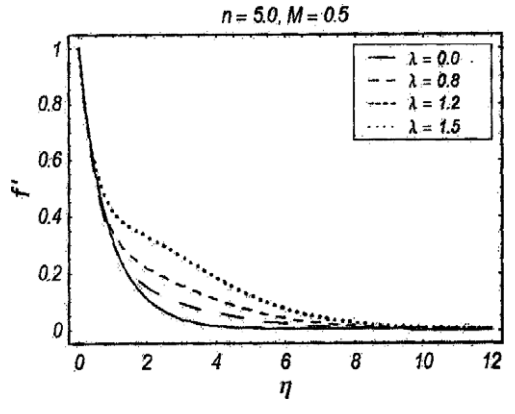

Fig. 4. Effects of λ on f' at $\hbar_1 = -0.6$.

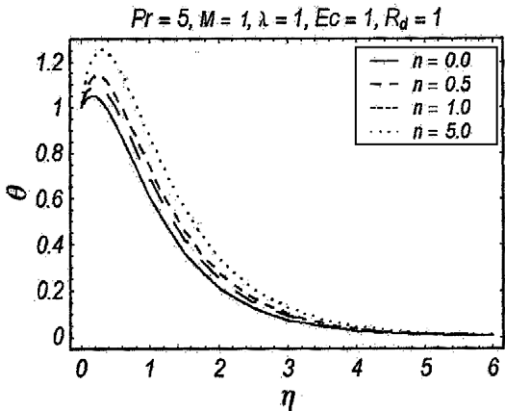

Fig. 5. Effects of n on θ at $\hbar_2 = -0.8$ for CST case.

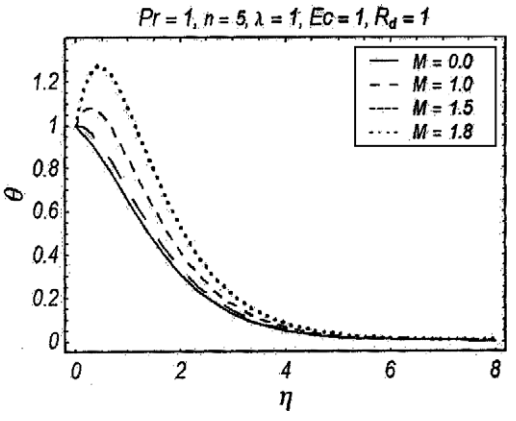

Fig. 6. Effects of M on θ at $\hbar_2 = -0.8$ for CST case.

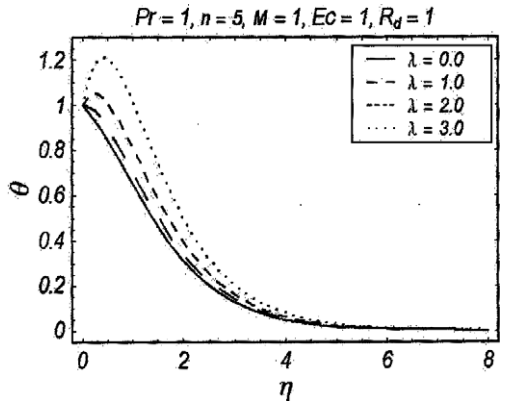

Fig. 7. Effects of λ on θ at $\hbar_2 = -0.8$ for CST case.

Tables 1–4 have been made in order to show the variations of wall shear stress $-f''(0)$ and the heat transfer characteristics at the wall $-\theta'(0)$ for different values of involving parameters. Table 1 gives the variations of n on the wall shear stress $-f''(0)$ when $(M = \lambda = 0)$. The magnitude of shear stress increases as n increases and the HAM solution has good agreement with the numerical solution [9]. Table 2 shows the values of $-f''(0)$ for different values of n, M and λ. The magnitude of the shear stress is increased for large values of n, M and λ. Tables 3 and 4 illustrate the heat

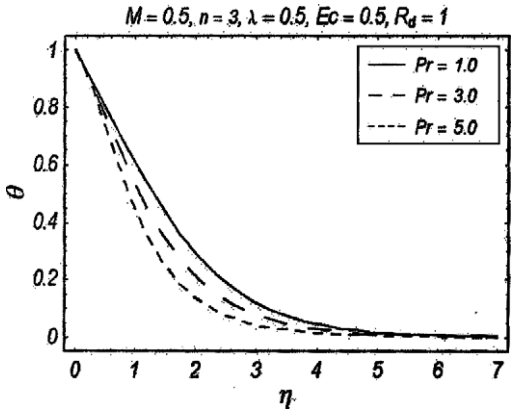

Fig. 8. Effects of Pr on θ at $\hbar_2 = -0.8$ for CST case.

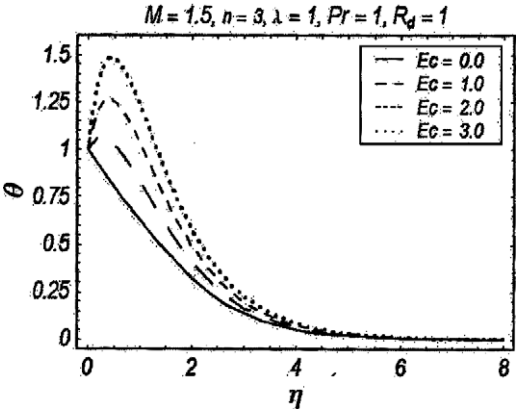

Fig. 9. Effects of Ec on θ at $\hbar_2 = -0.8$ for CST case.

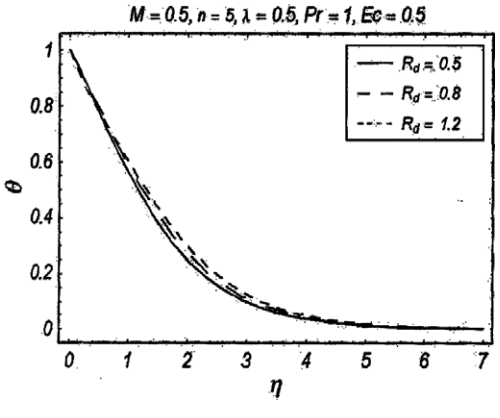

Fig. 10. Effects of R_d on θ at $\hbar_2 = -0.8$ for CST case.

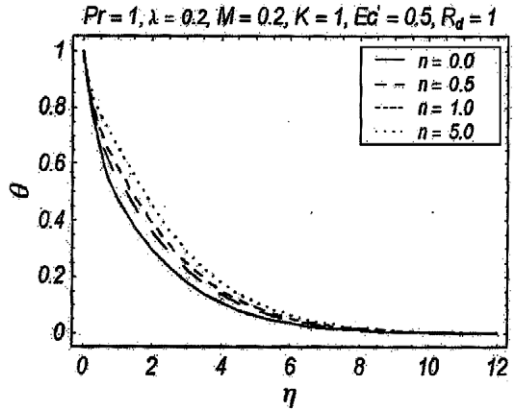

Fig. 11. Effects of n on θ at $\hbar_2 = -0.8$ for PST case.

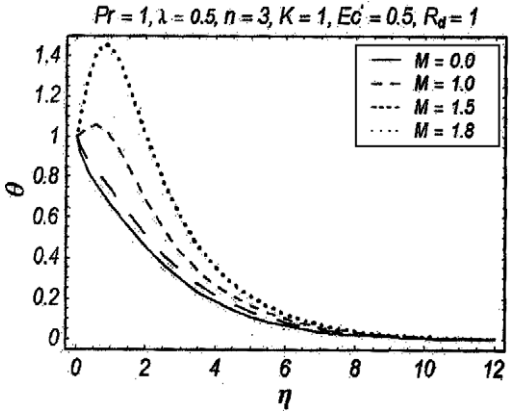

Fig. 12. Effects of M on θ at $\hbar_2 = -0.8$ for PST case.

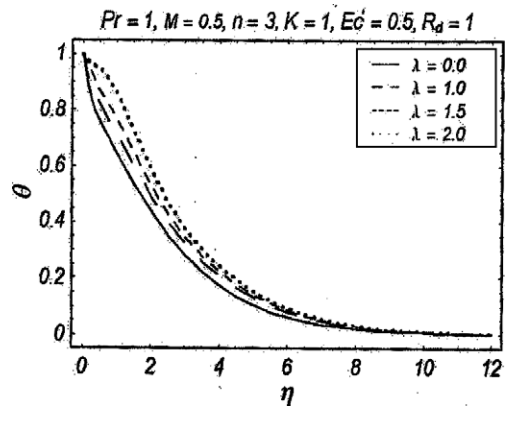

Fig. 13. Effects of λ on θ at $\hbar_2 = -0.8$ for PST case.

transfer characteristics at the wall $-\theta'(0)$ when ($M = \lambda = R_d = 0$) in CST and PST cases, respectively. Table 3 shows that the magnitude of $-\theta'(0)$ decreases for large values of n and increases as Pr increases for ($Ec = 0$ and $Ec \neq 0$). The magnitude of $-\theta'(0)$ increases for large values of n and Pr for ($Ec' = 0$ and $Ec' \neq 0$) in Table 4. From these tables one can see that the HAM solution has good agreement with the numerical solution [9] for both cases of CST and PST.

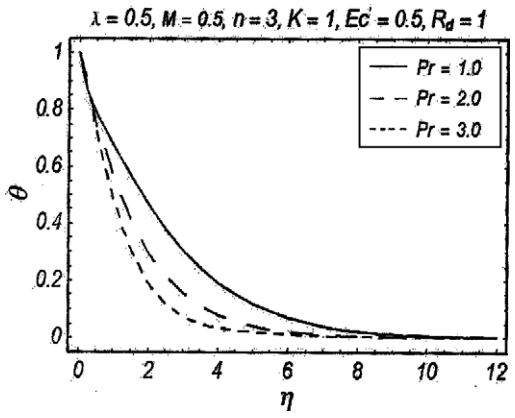

Fig. 14. Effects of Pr on θ at $\hbar_2 = -0.8$ for PST case.

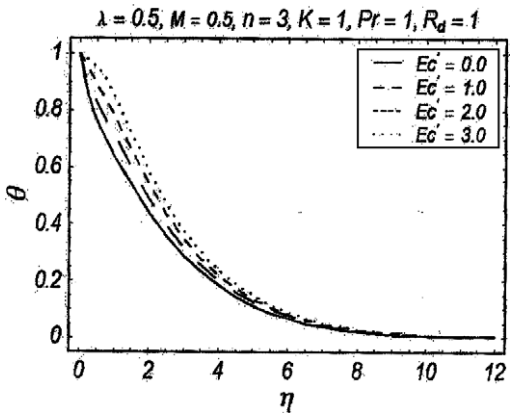

Fig. 15. Effects of Ed on θ at $\hbar_2 = -0.8$ for PST case.

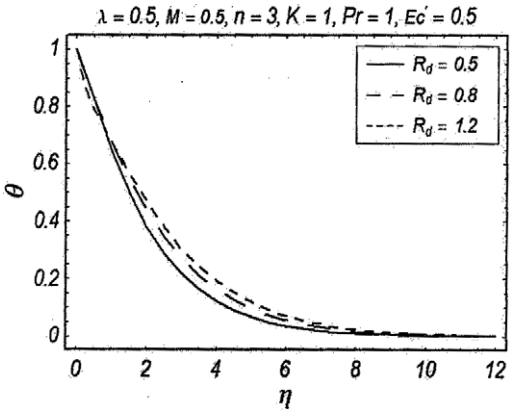

Fig. 16. Effects of R_d on θ at $\hbar_2 = -0.8$ for PST case.

7. Conclusions

In this analysis the effects of radiation on MHD flow of a viscous fluid with heat transfer is investigated. Series solutions for velocity and temperature fields are first developed and then discussed for various emerging parameters. The values of wall shear stress and heat transfer at the wall are also tabulated. The following observations have been made from the present analysis.

- The velocity f' and temperature θ increase for large values of n, M, λ, Ec, Ec' and R_d.
- The temperature θ decreases as Pr increases.
- The magnitude of the wall shear stress $-f''(0)$ increases as n, M and λ increases.
- The magnitude of $-\theta'(0)$ increases for large values of n and Pr and decreases for large vales of n in GST case.
- Tables 1, 3 and 4 show that HAM solution has good agreement with the numerical solution [9].

References

[1] B.C. Sakiadis, Boundary-layer behaviour on continuous solid surfaces, AIChE J. 7 (1961) 26–28.
[2] K. Sadeghy, A.H. Najafi, M. Saffaripour, Sakiadis flow of an upper-convected Maxwell fluid, Int. J. Non-Linear Mech. 40 (2005) 1220–1228.
[3] P.D. Ariel, T. Hayat, S. Asghar, The flow of an elasto-viscous fluid past a stretching sheet with partial slip, Acta Mech. 187 (2006) 29–35.
[4] S.J. Liao, An analytic solution of unsteady boundary-layer flows caused by an impulsively stretching plate, Commun. Non-linear Sci. Numer. Simul. 11 (2006) 326–339.
[5] H. Xu, An explicit analytic solution for convective heat transfer in an electrically conducting fluid at a stretching surface with uniform free stream, Int. J. Eng. Sci. 43 (2005) 859–874.
[6] R. Cortell, Effects of viscous dissipation and work done by deformation on the MHD flow and heat transfer of a viscoelastic fluid over a stretching sheet, Phys. Lett. A 357 (2006) 298–305.
[7] R. Cortell, Flow and heat transfer of a fluid through a porous medium over a stretching surface with internal heat generation/absorption and suction/blowing, Fluid Dyn. Res. 37 (2005) 231–245.
[8] R. Cortell, A note on flow and heat transfer of a viscoelastic fluid over a stretching sheet, Int. J. Non-Linear Mech. 41 (2006) 78–85.
[9] R. Cortell, Viscous flow and heat transfer over a nonlinearly stretching sheet, Appl. Math. Comput. 184 (2007) 864–873.
[10] S.J. Liao, Beyond perturbation, Introduction to homotopy analysis method, Chapman and Hall/CRC Press, Boca Raton, 2003.
[11] S.J. Liao, A uniformly valid analytic solution of 2D viscous flow past a semi-infinite flat plate, J. Fluid Mech. 385 (1999) 101–128.
[12] S.J. Liao, On the homotopy analysis method for nonlinear problems, Appl. Math. Comput. 147 (2004) 499–513.
[13] S.J. Liao, K.F. Cheung, Homotopy analysis of nonlinear progressive waves in deep water, J. Eng. Math. 45 (2003) 105–116.
[14] S.J. Liao, Comparison between the homotopy analysis method and homotopy perturbation method, Appl. Math. Comput. 169 (2005) 1186–1194.
[15] S. Abbasbandy, The application of homotopy analysis method to nonlinear equations arising in heat transfer, Phys. Lett. A 360 (2006) 109–113.
[16] Y. Tan, S. Abbasbandy, Homotopy analysis method for quadratic Recati differential equation, Commun. Non-linear Sci. Numer. Simul., in press.
[17] S.P. Zhu, An exact and explicit solution for the valuation of american put options, Qunatitat. Finance 6 (2006) 229–242.
[18] S.P. Zhu, A closed-form analytical solution for the valuation of convertible bonds with constant dividend yield, Anziam J. 47 (2006) 477–494.
[19] Y. Wu, C. Wang, S.J. Liao, Solving solitary waves with discontinuity by means of the homotopy analysis method, Choas Solitons & Fractals 26 (2005) 177–185.
[20] T. Hayat, T. Javed, M. Sajid, The influence of Hall current on rotating flow of a third grade fluid in a porous medium, J. Porous Media 10 (2007) 807–820.
[21] T. Hayat, M. Khan, M. Ayub, On the explicit analytic solutions of an Oldroyd 6-constant fluid, Int. J. Eng. Sci. 42 (2004), 123–135.

[22] T. Hayat, M. Khan, S. Asghar, Homotopy analysis of MHD flows of an Oldroyd 8-constant fluid, Acta Mech. 168 (2004) 213–232.
[23] M. Sajid, T. Hayat, S. Asghar, On the analytic solution of steady flow of a fourth grade fluid, Phys. Lett. A 355 (2006) 18–24.
[24] Z. Abbas, M. Sajid, T. Hayat, MHD boundary layer flow of an upper-convected Maxwell fluid in porous channel, Theor. Comput. Fluid Dyn. 20 (2006) 229–238.
[25] T. Hayat, Z. Abbas, M. Sajid, S. Asghar, The influence of thermal radiation on MHD flow of a second grade fluid, Int. J. Heat Mass Transfer 50 (2007) 931–941.
[26] T. Hayat, Z. Abbas, M. Sajid, Series solution for the upper-convected Maxwell fluid over a porous stretching plate, Phys. Lett. A 358 (2006) 396–403.
[27] M. Sajid, T. Hayat, S. Asghar, Comparison of the HAM and HPM solutions of thin film flows of non-Newtonian fluids on a moving belt, Nonlin. Dyn., in press.
[28] T. Hayat, M. Sajid, On analytic solution for thin film flow of a fourth grade fluid down a vertical cylinder, Phys. Lett. A 361 (2007) 316–322.
[29] T. Hayat, M. Khan, M. Ayub, Couette and Poiseuille flows of an Oldroyd 6-constant fluid with magnetic field, J. Math. Anal. Appl. 298 (2004) 225–244.
[30] T. Hayat, Z. Abbas, Heat transfer analysis on the MHD flow of a second grade fluid in a channel with porous medium, Choas Solitons & Fractals, in press.
[31] T. Hayat, Z. Abbas, M. Sajid, MHD stagnation-point flow of an upper-convected" Maxwell fluid over a stretching surface, Choas Solitons & Fractals, in press.
[32] M. Khan, Z. Abbas, T. Hayat, Analytic solution for flow of Sisko fluid through a porous medium, Transport Porous Media, in press.
[33] F.M. Allan, Derivation of the Adomian decomposition method using the homotopy analysis method, Appl. Math. Comput. 190 (2007) 6–14.
[34] J.A. Shercliff, A text Book of Magnetohydrodynamics, Pergamon Press, Elmsford, New York, 1965.
[35] G.W. Sutton, A. Sherman, Engineering Magnetohydrodynamic, McGraw Hill, New York, 1965.
[36] M.M. Ali, T.S. Chen, B.F. Armaly, Natural convection-radiation interaction in boundary layer flow over horizontal surfaces, AIAA J. 22 (1984) 1797–1803.